https://doi.org/10.5194/egusphere-2026-4918
Preprint. Discussion started: 31 August 2026

Combining an individual–based dynamic vegetation model with a distributive hydrologic model to improve coupled water–carbon modelling

Niklas Bruns[1], Andreas Huth[1, 2, 3], Stephan Thober[4], and Samuel M. Fischer[1]

[1]Helmholtz Center for Environmental Research – UFZ, Leipzig, Germany, Department of Ecological modelling
[2]Institute for Environmental Systems Research, University of Osnabrück, Osnabrück, Germany
[3]iDiv German Centre for Integrative Biodiversity Research Halle-Jena-Leipzig, Leipzig, Germany
[4]Helmholtz Center for Environmental Research – UFZ, Leipzig, Germany, Department of Computational Hydrosystems

Correspondence: Niklas Bruns (niklas.bruns@ufz.de)

Abstract. Vegetation and hydrology are tightly coupled: forest structure regulates evapotranspiration and soil moisture, while water availability governs tree growth, mortality, and succession. Yet hydrological and dynamic vegetation models typically maintain a domain-specific focus, limiting their ability to represent the feedbacks between forest dynamics and catchment-scale water dynamics. We address this gap by coupling the distributed hydrological model mHM with the individual-based forest model FORMIND, and apply the coupled framework (FORMIND-mHM) to the Selke river catchment in Central Germany, a mixed deciduous catchment with approximately 40 % forest cover. We examine how explicit vegetation–water interactions affect hydrological flux partitioning, and whether catchment-scale discharge carries exploitable information about stand-scale gross primary production (GPP). The coupled framework achieved discharge performance comparable to stand-alone mHM while substantially altering ET partitioning, shifting the transpiration fraction (E_t/ET) from 0.50 in stand-alone mHM to 0.73 in the coupled framework, closer to observed ranges for temperate forests. Furthermore, a seasonal GPP–discharge relationship emerged consistently across all gauges, demonstrating that river discharge carries information about forest productivity, an analytical pathway accessible only through coupled modelling. FORMIND-mHM is therefore particularly suited to applications where vegetation–water feedbacks are central, including long-term projections of forest dynamics under changing climatic conditions.

1 Introduction

The vegetation and the hydrological cycles of landscapes are tightly coupled (Beaulieu et al., 2016). Forest structure and composition regulate evapotranspiration, interception, and soil moisture dynamics (Andréassian, 2004; Ellison et al., 2017), while water availability governs tree growth, mortality, and successional trajectories (Allen et al., 2010; Choat et al., 2012; Wang et al., 2019). These interactions and feedbacks are inherently bidirectional and operate across both short and long timescales (Fatichi et al., 2016a; Wang et al., 2019). Understanding them is fundamental to predicting how forests and water balances respond to environmental change.

Well-established models exist for both domains and have been successfully applied across a broad range of research questions. Forest models are widely used to investigate forest properties such as carbon balance, tree size distributions, and successional dynamics, processes that are otherwise difficult to study due to challenges of spatial scale and observational timescales (Bugmann and Seidl, 2022; Fischer et al., 2025). With increasing pressures from ongoing climate change, intensifying disturbance regimes, shifting societal demands on forest ecosystems, and growing challenges in reforestation and forest management, forest models are used for addressing several pressing questions facing forest ecosystems today (Shifley et al., 2017; Bugmann and Seidl, 2022; Seidl and Turner, 2022; Díaz-Yáñez et al., 2024). Hydrological models, in turn, are broadly applied for understanding water fluxes at the catchment scale, with applications ranging from flood forecasting to drought monitoring and water resource management (Sahu et al., 2023). As climate change alters precipitation patterns (Drollinger et al., 2025) and intensifies hydrological extremes (Boeing et al., 2025; Swain et al., 2025) while global water demand continues to grow (Wada et al., 2013), hydrological models are increasingly relied upon to inform water management under conditions that differ substantially from the historical record (Fatichi et al., 2016b).

However, due to their respective domain-specific foci, both forest models and hydrological models often come with complementary limitations that constrain their ability to represent the feedbacks between forest dynamics and catchment-scale water cycling (Fatichi et al., 2016a; Wang et al., 2019; Zhang et al., 2023). While some global vegetation models, such as LPJml, are being applied to examine hydrologic fluxes (Zaherpour et al., 2018), many stand-scale forest models use simplified representations of soil water dynamics. While vegetation structure and productivity are influenced by water availability, the hydrological processes that determine soil moisture, including infiltration, drainage, and lateral redistribution, are rarely represented in more detail (Fatichi et al., 2016a; Bugmann and Seidl, 2022). This potentially limits the ability of forest models to capture how vertical and catchment-scale heterogeneity in soil moisture constrains tree water uptake and growth, particularly under conditions where water availability is a primary driver of forest dynamics. Hydrological models, conversely, often simplify plant–water interactions, relying on empirical methods to calculate potential evapotranspiration and prescribing static values of leaf area index (LAI) as a proxy for vegetation. Ecophysiological processes such as photosynthesis, transpiration, and respiration are integral to the hydrological cycle and highly dynamic, responding to climate variability, disturbances, and environmental stressors (Thompson et al., 2011; Kordrostami et al., 2025). Given the dominance of transpiration in continental evapotranspiration, Jasechko et al. (2013) argue that improvements in the simulation of biological water fluxes should be prioritised over physical evaporation fluxes in hydrological modelling. Conventional hydrological models therefore systematically miss the influence of vegetation dynamics, both long-term structural changes and short-term physiological responses, on water flux partitioning (Kim et al., 2018).

As a result, key emergent properties of coupled water-vegetation systems, including the partitioning of evapotranspiration, the regulation of soil moisture, and the translation of vegetation dynamics into catchment-scale water fluxes are difficult to assess via these domain-specific models, limiting their ability to represent the coupled behaviour of water and vegetation systems. Parameters governing cross-domain processes, such as plant water use efficiency, which directly links carbon assimilation to water loss, are particularly difficult to constrain from single-domain observations alone.

https://doi.org/10.5194/egusphere-2026-4918
Preprint. Discussion started: 31 August 2026

Representing these dynamic vegetation–soil moisture feedbacks in environmental models requires a joint modelling approach. As the construction of monolithic interdisciplinary models pose great scientific and technical challenges (Vedder et al., 2024), we chose to couple existing models using the FINAM model coupling Framework (Müller et al., 2025). Specifically, we couple a process-based individual-based forest model with a distributed hydrological model, combining the strengths of both domains to provide a more process-consistent representation of vegetation–water feedbacks: a hydrological soil module provides the forest model with a detailed and spatially consistent representation of soil moisture, while explicit vegetation dynamics replace the static parametrisations of the hydrological model with a physiologically grounded representation of plant water use.

For the vegetation component, we use FORMIND (Köhler and Huth, 1998; Bohn et al., 2014; Fischer et al., 2016), a dynamic vegetation model of the forest gap model class that simulates forest dynamics by explicitly representing individual trees within patches of $20\,\mathrm{m} \times 20\,\mathrm{m}$. Applications range from stand-scale analyses of forest structure and carbon cycling at the hectare scale to ecosystem-scale investigations of tropical forest dynamics across regions such as the Amazon basin (Rödig et al., 2017a, 2019; Bauer et al., 2021, 2024). Soil water availability is a central driver within the model, as spatial heterogeneity in soil moisture at the patch scale strongly influences emergent forest structure and productivity, yet the hydrological processes governing soil moisture availability remain simplified within the model, motivating the coupling approach pursued in this study.

For the hydrological component, we use the spatially distributed mesoscale hydrologic model mHM (Samaniego et al., 2010; Kumar et al., 2013; Thober et al., 2019), which simulates key processes of the hydrologic cycle using a grid-based approach that accounts for spatial heterogeneity in topography, land use, and soil type. The model operates at grid resolution ranging from $1\,\mathrm{km} \times 1\,\mathrm{km}$ to $4\,\mathrm{km} \times 4\,\mathrm{km}$. In this study, we set the cell size at the intermediate level to $4\,\mathrm{km} \times 4\,\mathrm{km}$ compatible with the German drought monitor (Zink et al., 2016). Vegetation in mHM is represented through prescribed LAI values, which define canopy storage capacity and regulate evapotranspiration potential. This static representation, while computationally efficient, cannot capture the dynamic feedbacks between forest structure and hydrological partitioning that are the focus of this study.

Coupling independently developed domain-specific models is a challenging task and gives rise to both methodological questions regarding the coupling as well as analytical questions concerning the dynamics of the joint model, which we address in this paper. The considered models operate on vastly different spatial scales and differ in their representation of vegetation and hydrological processes. We therefore ask (1) how the spatial and process-level differences between an individual-based forest model and a mesoscale hydrological model can be reconciled within a coupled modelling framework, (2) examine how the coupling affects the partitioning of water fluxes, and (3) analyse whether it improves the representation of key hydrological processes compared to stand-alone approaches. Building on this, the coupled framework opens new analytical possibilities that neither stand-alone model can provide. To demonstrate these capabilities, we (4) analyse to what extent hydrological signals at the catchment scale carry information about carbon cycle dynamics at the stand scale and apply the framework for cross-domain parameter inference. By addressing these questions, this work aims to demonstrate the value of explicit water–vegetation coupling for improving process understanding, enabling cross-domain model parametrization, and advancing predictions of ecohydrological dynamics under environmental change.

https://doi.org/10.5194/egusphere-2026-4918
Preprint. Discussion started: 31 August 2026

We apply the coupled model framework as a case study to the Selke catchment in Central Germany ($458\,\mathrm{km}^2$) and use observations from two complementary sites within the Terrestrial Environmental Observatories (TERENO) network for model validation. Leveraging inventory data and eddy covariance measurements from the 'Hohes Holz' site, a mixed deciduous forest in Central Germany, we validate the vegetation component of the coupled model framework under well- characterized climatic and forest conditions. The hydrological component of the coupling is validated using discharge observations from three gauges within the Selke catchment, which extends across the forested Harz Mountains and the predominantly agricultural foreland. Subsequently, we apply the complete coupled modelling framework to the Selke catchment, offering insights into vegetation–hydrology interactions across the full range of land cover conditions present in the catchment.

2 Methods

To analyse the effect of dynamic vegetation on soil moisture dynamics and catchment-scale hydrology, we coupled the individual-based forest gap model FORMIND with the mesoscale hydrological model mHM using the FINAM model coupling framework (Müller et al., 2025). We applied the coupled framework at two complementary scales: at the stand scale, evaluating its performance against eddy covariance measurements at the $9\,\mathrm{ha}$ 'Hohes Holz' mixed deciduous forest site in Central Germany, and at the catchment scale, applying the complete framework to the Selke catchment in the Harz Mountain region. The following sections introduce each model component, describe the coupling architecture, the model evaluation at both study sites, the model setup for the Selke catchment, and finally provide an overview of the experiments conducted at both scales.

2.1 Forest model FORMIND

FORMIND is a process-based, dynamic vegetation model belonging to the forest gap model family, which has been continuously developed since the late 1990s (Shugart et al., 2018). The model simulates forest dynamics by explicitly representing individual trees within $20\,\mathrm{m} \times 20\,\mathrm{m}$ patches, capturing tree growth, mortality, recruitment, and competition for light, canopy space, and water (Rödig et al., 2017b; Holtmann et al., 2021).

Soil water availability is a central driver of forest structure in FORMIND. Heterogeneity in soil moisture at the patch level influences structural diversity in modelled forests through its effect on gross primary productivity (GPP). First, the potential GPP of the forest achievable under optimal temperature and sufficient soil water conditions is computed based on incoming radiation. Plant water uptake is assumed to be proportional to GPP (water use efficiency concept) but constrained by three factors: the maximal atmospheric water demand, the amount of water available in the soil, and the competition between trees for water resources. GPP is then adjusted according to the actual amount of water absorbed using a GPP reduction factor. The

https://doi.org/10.5194/egusphere-2026-4918
Preprint. Discussion started: 31 August 2026

reduction factor is calculated using the approach of Granier et al. (1999) as follows:

$$\varphi_w(\Theta_{\text{soil}}) = \begin{cases} 0 & \text{if } \Theta_{\text{soil}}(t) \leq \Theta_{\text{pwp}}, \\ \dfrac{\Theta_{\text{soil}}(t) - \Theta_{\text{pwp}}}{\Theta_{\text{msw}} - \Theta_{\text{pwp}}} & \text{if } \Theta_{\text{pwp}} < \Theta_{\text{soil}}(t) \leq \Theta_{\text{msw}}, \\ 1 & \text{if } \Theta_{\text{msw}} < \Theta_{\text{soil}}(t), \end{cases} \tag{1}$$

where Θ_{pwp} is the permanent wilting point in $V\,\%$ and Θ_{msw} is the minimum soil water content in $V\,\%$ (Rödig et al., 2017b). FORMIND's soil water compartment consists of a single soil layer of configurable depth, set to 2 m for temperate forests in this study. Daily soil water content depends on precipitation (PR), interception (IN), plant water uptake (TR), and surface and subsurface runoff (RO):

$$\frac{d\Theta_{\text{soil}}}{dt} = PR(t) - IN(t) - RO(t) - TR(t). \tag{2}$$

Interception is calculated as a function of leaf area index (LAI); surface runoff depends on the amount of water already pooling and on soil porosity; gravitational subsurface runoff is calculated using the Brooks–Corey relation as implemented in Liang et al. (1994); and transpiration is calculated using the water-use-efficiency concept:

$$TR = \frac{1}{A_{\text{patch}}} \sum_{\text{all trees}} \frac{\text{GPP}}{\text{WUE}}, \tag{3}$$

where A_{patch} is the patch size in m^2. As soil water content is tracked independently for each patch, surface and subsurface runoff that exits a patch does not contribute to the water balance of neighboring patches. The water balance is therefore closed at the patch scale, but not at the ecosystem or catchment scale.

2.2 Mesoscale hydrologic model mHM

The mesoscale Hydrological Model (mHM) (Samaniego et al., 2010; Kumar et al., 2013; Thober et al., 2019) is a grid-based, spatially explicit hydrologic model accounting for canopy interception, snow accumulation and melt, soil moisture dynamics, infiltration and surface runoff, evapotranspiration, subsurface storage and discharge generation, deep percolation and base flow, as well as flood routing. The model employs a multiscale parameter regionalisation scheme to account for the variability of landscape attributes and model parameters at the sub-grid level, thereby enabling seamless prediction of water flows and conditions across different spatial scales and locations. In this study, we set the cell size at the intermediate level to $4\,\text{km} \times 4\,\text{km}$ compatible with the German drought monitor (Zink et al., 2016).

In mHM, vegetation is represented by prescribed monthly values of leaf area index (LAI) that vary seasonally but remain constant across years. The LAI determines the canopy interception storage and, depending on model configuration, is used to estimate a correction term to the potential evapotranspiration (PET). Soil moisture dynamics are resolved across k discrete soil layers within the root zone, collectively referred to as the upper soil. Actual evapotranspiration from the kth soil layers, E_3^k, is calculated based on soil moisture stress, the fraction of roots present, and the remaining PET. We follow the notation of Samaniego et al. (2010), where subscript numbers on β denote the specific parameter as introduced in the original publication:

https://doi.org/10.5194/egusphere-2026-4918
Preprint. Discussion started: 31 August 2026

$$E_3^k(t) = \begin{cases} \alpha^k \beta_{17}^k \left(E_p^{'}(t)\right) & \text{if } k = 1, \\ \alpha^k \beta_{17}^k \left(E_p^{'}(t) - \sum_{n=1}^{k-1} E_3^{k-1}(t)\right) & \text{otherwise,} \end{cases} \quad (4)$$

with

$$E_p^{'}(t) = E_p(t) - E_1(t) - E_2(t), \quad (5)$$

where E_p is the potential evapotranspiration, $E_1(t)$ is evaporation from the canopy in $\mathrm{mm\,d^{-1}}$, $E_2(t)$ is evaporation from free-water bodies in $\mathrm{mm\,d^{-1}}$, and β_{17}^k is the fraction of roots in layer k. For the coupled framework we assume a constant PET throughout all soil layers. The soil moisture stress factor α^k is defined as:

$$\alpha^k = \begin{cases} 0 & \text{if } x_3^k(t-1) \leq \beta_{15}^k, \\ \dfrac{x_3^k(t-1) - \beta_{15}^k}{\beta_{16}^k - \beta_{15}^k} & \text{if } \beta_{15}^k < x_3^k(t-1) \leq \beta_{16}^k, \\ 1 & \text{otherwise,} \end{cases} \quad (6)$$

where $x_3^k(t-1)$ is the soil moisture in layer k at the previous time step, β_{15}^k is the permanent wilting point, and β_{16}^k is the soil moisture limit above which actual transpiration is equated with PET. This formulation is structurally equivalent to the soil moisture stress function used in FORMIND (Eq. (1)), allowing both models to respond consistently to soil water limitation despite operating with different vertical soil discretizations.

The remaining net rainfall, after accounting for interception, is partitioned into soil moisture storage and infiltration into the root zone layers. Total runoff generated at each cell consists of fast and slow interflow components and base flow, and is routed to the downstream neighboring cell.

2.3 Coupling components and implementation.

FORMIND and mHM are usually applied to different spatial domains and scales. FORMIND simulates forest dynamics and is therefore only applied to forested areas, whereas mHM is designed to simulate the complete water balance of entire catchments. Coupling the two models therefore required reconciling two spatial domains that only partially overlap, one being the catchment as a whole, and the other the subset of forested grid cells within it for which FORMIND provides vegetation dynamics. We addressed this challenge by explicitly separating model components by their spatial domain and scale. We simulated forested areas using the coupled FORMIND–mHM system at the patch scale ($20\,\mathrm{m} \times 20\,\mathrm{m}$), while the mHM component continued to simulate non-forested areas on a $4\,\mathrm{km} \times 4\,\mathrm{km}$ grid; we subsequently combined the output of the two domains to obtain catchment-wide water fluxes. For each $4\,\mathrm{km} \times 4\,\mathrm{km}$ grid cell, we considered a sample of $9\,\mathrm{ha}$ of forest, i.e., 225 individual patches, each with its own soil moisture storage (Figure 1).

In the coupled model framework (FORMIND-mHM), we wrapped each included model in a so-called 'FINAM component'. Such components exhibit a well-specified interface, which facilitates the data exchange between them (Müller et al., 2025).

https://doi.org/10.5194/egusphere-2026-4918
Preprint. Discussion started: 31 August 2026

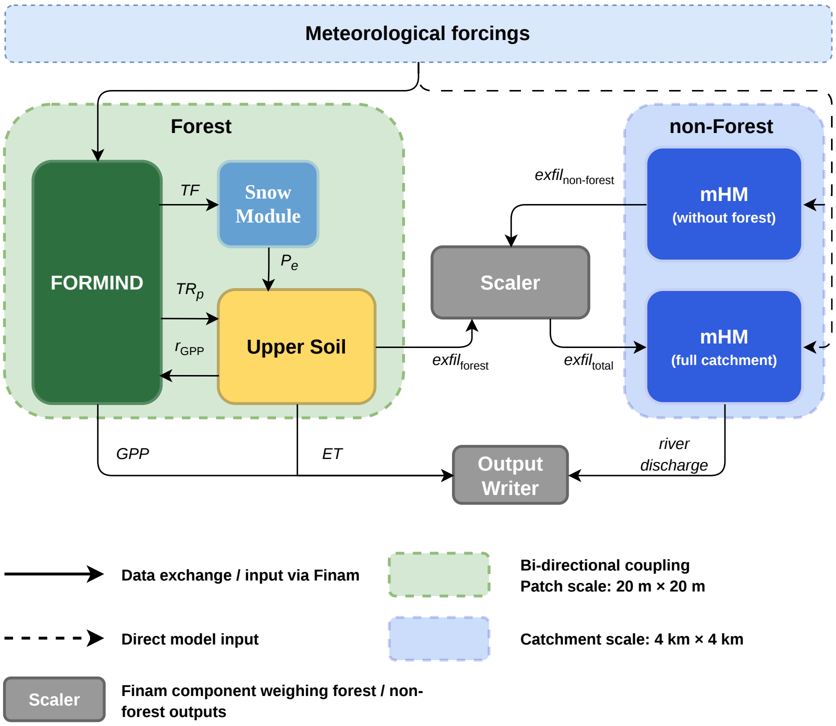

Figure 1. Conceptual overview of the coupled model framework including the forest model FORMIND, the hydrologic model mHM and the model coupling framework FINAM. FORMIND and the upper soil component are engaged in a circular coupling on $20\,\text{m} \times 20\,\text{m}$ patches. The mHM instances are running on a $4\,\text{km} \times 4\,\text{km}$ grid. Output from forest and non-forest is weighted by land cover fractions in a scaling component and passed to the catchment-wide mHM component. The data passed between components are as follows: throughfall (TR), effective precipitation (P_e), potential transpiration (TR_p), GPP reduction factor (r_{GPP}), forest ($exfil_{forest}$) and non-forest exfiltration ($exfil_{non\text{-}forest}$) and total exfiltration into the lower soil ($exfil_{total}$). Output variables, including daily values of GPP (FORMIND), ET (upper soil), and river discharge (mHM full-catchment), are written to NetCDF format via a dedicated output writer component integrated into the FINAM framework.

https://doi.org/10.5194/egusphere-2026-4918
Preprint. Discussion started: 31 August 2026

Implementing the separation of forested and non-forested domains within this framework required six components, which we grouped into three functional categories: main components, scale-transferred process components, and a scaling component.

The three main model components were the FORMIND component for forest dynamics; an mHM component for water dynamics in non-forested areas; and an mHM component for runoff estimation and river routing in the complete catchment. The FORMIND component modelled forest dynamics at patch-scale for all forested areas and calculated tree water demand. The mHM component for water dynamics calculated soil moisture dynamics at grid-scale for all non-forested areas. The mHM component for the complete catchment received infiltration fluxes into the lower soil from forested and non-forested areas and modelled catchment-wide subsurface flows and river discharge.

Two additional scale-transferred process components brought processes originally represented at the mHM grid scale ($4\,\mathrm{km} \times 4\,\mathrm{km}$) down to the scale of individual forest patches ($0.04\,\mathrm{ha}$), namely a snow module and a soil moisture module. The soil module and the snow module were necessary to link the process representations of FORMIND and mHM at the patch scale. The soil component calculated actual evapotranspiration and changes in soil moisture according to mHM principles (Eq. (4)), based on the water demand of trees calculated by the FORMIND component. We implemented it as a stand-alone component to provide each forest patch in FORMIND with its own soil moisture storage, explicitly linking the patch-scale vegetation dynamics of FORMIND with the grid-scale hydrology of mHM. Due to the sequential calculation of hydrologic processes in mHM, we also implemented the snow module as an independent FINAM component, calculating snow accumulation and melt for each patch. Both components were implemented following the structure and logic of their respective mHM counterparts (Samaniego et al., 2010; Kumar et al., 2013).

Finally, we introduced a scaling component combining the exfiltration fluxes (infiltration into the lower soil) from the forested and non-forested domains according to land-cover fractions per $4\,\mathrm{km} \times 4\,\mathrm{km}$ cell (Eq. (7)) and passed the resulting catchment-wide exfiltration to the catchment-wide mHM component, which calculated all subsurface flows for the entire catchment.

The individual processes were simulated in the following order: for every simulated day, FORMIND first computed the potential transpiration (Eq. (3) and passed it to the soil module, which used it to calculate new soil moisture levels and derived a GPP reduction factor based on the mHM soil stress factor (Eq. (6)). FORMIND then applied this factor to adjust GPP estimates for the forest according to soil water limitations, accounting for interspecific competition for water and soil moisture availability. The soil module subsequently provided exfiltration for all forested areas to the scaling component, which combined it with the corresponding non-forested contribution from the mHM component for non-forested areas:

$$exfil_{\mathrm{total}} = f_{\mathrm{forest}} \cdot exfil_{\mathrm{forest}} + f_{\mathrm{notSealedNotForest}} \cdot exfil_{\text{non-forest}} \tag{7}$$

where f_{forest} is the fraction of the grid cell covered by forest, $f_{\mathrm{notSealedNotForest}}$ is the fraction of the cell that is neither covered by impermeable surfaces nor forested, $exfil_{\mathrm{forest}}$ is the exfiltration calculated by the soil module for the forested fraction, and $exfil_{\mathrm{non-forest}}$ is the exfiltration calculated by mHM for the non-forested fraction. Weighting the non-forest contribution by $f_{\mathrm{notSealedNotForest}}$ rather than the total non-forest fraction excluded sealed surfaces, from which no exfiltration into the lower

https://doi.org/10.5194/egusphere-2026-4918
Preprint. Discussion started: 31 August 2026

soil occurs. The catchment-wide mHM component acted solely as a receiver of this combined exfiltration input and continued to calculate subsurface flows and runoff generation for the entire catchment area.

2.4 Model evaluation and analysis

Since the coupled framework integrates two models from different modelling domains, we assessed its dynamics separately for each domain before evaluating the fully coupled system at the catchment scale. Therefore, we conducted the model evaluation in two parts. To that end, we used observations from two complementary research sites within the TERENO network: the Hohes Holz forest site, used to evaluate the vegetation component against eddy covariance measurements, and the Selke river catchment, used to evaluate the hydrological component against discharge observations from the Meisdorf gauging station.

The Selke catchment is situated in the Harz Mountain region and the Harz foreland in Saxony-Anhalt, Germany, covering an area of 458 km^2 with a main stream length of 64.4 km and a forest cover of approximately 40 $\%$ (Figure 2). It is a sub-catchment of the intensively monitored Bode catchment within the TERENO network. The upper Selke is located in the Harz Mountains, where forests dominate the landscape, followed by agricultural land. As the upper Selke is at a higher elevation, snowmelt contributes considerably to river discharge in late winter and spring. The downstream part of the catchment, hereafter called the 'Lower Selke', lies in the foreland of the Harz Mountains. The Lower Selke is a fertile plain with productive soils, dominated by arable agriculture (Winter et al., 2021).

2.4.1 Model setup for the Selke catchment

We set up both models for the Selke catchment using publicly available input data. We parametrised FORMIND using a temperate deciduous forest parameter set (Fischer et al., 2026), representing the mixed beech–oak forest conditions characteristic of the Selke catchment. We configured mHM using the German Drought Monitor setup (GDM-v1-2016) introduced by Boeing et al. (2022), providing soil texture, topography, and land cover data at the required spatial resolution.

We obtained meteorological forcing data, including daily precipitation, mean temperature, and minimum and maximum temperature, from the Deutsche Wetterdienst (DWD). We provided potential evapotranspiration (PET) as an external input, calculated using the Hargreaves–Samani method from the same meteorological data. The land cover data distinguishes forest, impervious, and pervious surfaces as the three land cover classes used in the coupled framework. We took soil hydraulic properties and geological information from GDM-v1-2016, and obtained observed stream flow data for model evaluation operated by the Landesbetrieb für Hochwasserschutz und Wasserwirtschaft Sachsen-Anhalt (LHW). The initialization of the forest component was based on 1 km × 1,km inventories extrapolated from forest inventory data from the German National Forest Inventory, which we processed as described below.

For each 4 km × 4 km mHM grid cell with a forest fraction above 5 $\%$, we identified the nearest 1 km × 1,km inventory point within 4 km using a KDTree spatial search and selected the inventory with the highest forest fraction as the representative initialization. Since we ran FORMIND on a representative 300 m × 300 m simulation area in each mHM grid cell, we subsampled each 1 km × 1,km inventory by dividing it into a 3 × 3 grid of 300 m × 300 m tiles and selected the tile with the

https://doi.org/10.5194/egusphere-2026-4918
Preprint. Discussion started: 31 August 2026

highest tree density. We shifted tree coordinates to the tile origin prior to model initialization. We initialized grid cells without a suitable inventory within the search radius using a default inventory representative of the broader study area.

2.4.2 Stand-scale evaluation

To assess the functionality of the vegetation component at the stand-scale, we compared daily ET and GPP estimates from both FORMIND-mHM and stand-alone FORMIND against eddy covariance observations, and evaluated the performance of the coupled framework relative to the stand-alone model. To that end, we applied both models to the Hohes Holz forest and initialized them with the same 9 ha of forest inventory data from the site. Furthermore, we applied the same mode parametrization, using soil parameters adjusted according to the local soil type (Maidment, 1995). We used observational data from an eddy covariance tower situated at the forest site (Pohl et al., 2023) and compared daily ET and GPP estimates from both models against tower observations using linear regression.

The forest research site 'Hohes Holz' is located within a mixed deciduous forest situated 200 metres above sea level in the Magdeburger Boerde region of Central Germany (52° 05′ N, 11° 13′ E). It has a subatlantic-submontane climate, with an average annual temperature of 9.1 °C and an average annual precipitation of 563 mm in the climatic period 1981– 2010. The study site is dominated by European beech (*Fagus sylvatica L.*) and sessile oak (*Quercus petraea*) and lies within a 15 km^2 area of predominantly municipal forest, which is managed by regional forestry. The 'Hohes Holz' study site was established in 2013 as part of the TERENO project (Pohl et al., 2023).

2.4.3 Catchment-scale evaluation

To assess the plausibility of the hydrological component at the catchment-scale, we compared discharge simulations from the coupled framework as well as a stand-alone version of mHM and the observed stream flow in the Selke catchment. Three gauges measure river discharge within the Selke catchment: Hausneindorf, Meisdorf, and Silberhütte, ordered from downstream to upstream. We focused model evaluation on gauge Meisdorf, which drains a sub-catchment with a higher forest cover fraction than the full catchment represented by Hausneindorf, making it more directly relevant for assessing the effect of dynamic vegetation on hydrological partitioning. We evaluated daily discharge simulations from both model configurations against observations using the Kling-Gupta Efficiency (KGE) and its components (correlation r, variability ratio α, and bias ratio β).

2.4.4 Model analysis

To assess the effect of both the coupling and parameter optimization on model performance, we evaluated four model configurations. The first configuration, mHM, represented stand-alone mHM with default parameters. The second configuration, FORMIND-mHM, represented the coupled framework with the same default parameters, allowing us to isolate the effect of the coupling. The third configuration, $\mathrm{mHM_{opt}}$, represented stand-alone mHM with parameters optimized for gauge Meisdorf. The fourth configuration, FORMIND-$\mathrm{mHM_{opt}}$, represented the coupled framework using the soil parameters derived from the $\mathrm{mHM_{opt}}$ optimization, allowing us to assess the effect of parameter optimization on the coupled framework without introduc-

https://doi.org/10.5194/egusphere-2026-4918
Preprint. Discussion started: 31 August 2026

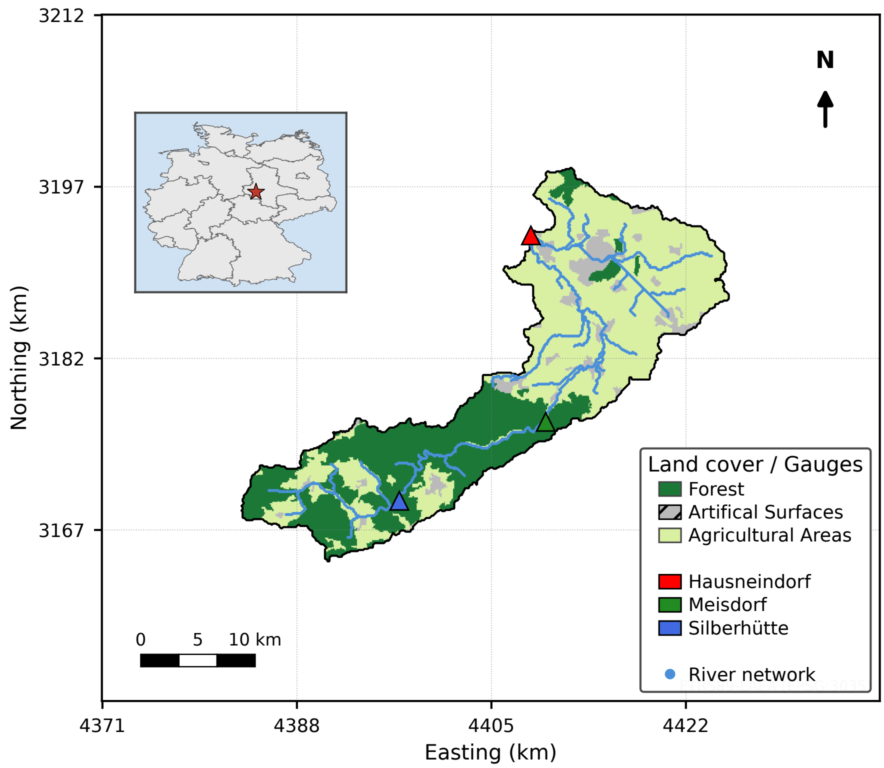

Figure 2. Catchment map of the Selke basin in central Germany. The catchment has an area of 458 km^2 with approximately 40 % forest cover. Land cover classes are presented as defined in mHM and are classified into forest (dark green), artificial surfaces (grey, hatched), and agricultural areas (light green). Triangles indicate the three stream gauges present in the catchment: Silberhütte (blue), Meisdorf (green), and Hausneindorf (red), ordered from upstream to downstream. The river network is derived from mHM.

ing additional degrees of freedom. We did not independently optimize FORMIND, as the coupled framework already achieved satisfactory agreement with observed GPP and ET at the Hohes Holz site using the existing temperate forest parametrization, and optimizing FORMIND against hydrological target variables risks conflating the contributions of the vegetation and hydrological components to overall model performance.

We further examined the sensitivity of the coupled framework to two key parameters, the canopy interception constant in mHM and the water use efficiency (WUE) in FORMIND, varying both parameters independently while holding all other parameters constant. We tested the canopy interception constant at four values corresponding to 25 %, 50 %, 75 %, and 100 % of the original parameter value, and WUE at five values ranging from 2 to 10 in increments of 2. We ran each configuration for the period 2005–2015 with a three year warm-up period and evaluated model performance using the KGE at gauge Meisdorf.

To assess the relationship between vegetation productivity and catchment-scale discharge, we conducted an interannual regression analysis between simulated GPP and observed discharge (Q) for all three gauges in the Selke catchment. Prior to

https://doi.org/10.5194/egusphere-2026-4918
Preprint. Discussion started: 31 August 2026

analysis, we smoothed both GPP and Q time series using a 7-day centered moving average to reduce high-frequency variability. We shifted GPP 15 days forward in time to account for the delay between vegetation water uptake and its subsequent expression in stream flow. We selected this lag based on a sensitivity test across values between 7 and 30 days, with 15 days producing the most consistent results across all three gauges. This value is broadly consistent with the characteristic timescale of the slow interflow component in mHM for the Selke catchment, as implied by the recession coefficient K_s, and falls within the range of vegetation water transit time estimates for temperate forests reported in the literature (Felton et al., 2025).

We then applied the following procedure for each day of year (DOY) separately. We computed the mean GPP and mean Q within a $\pm$7-day window around the respective DOY for each year individually, yielding one paired value per year for each DOY. We then calculated an interannual Pearson correlation coefficient (R) and regression slope across these annual values using linear regression, requiring a minimum of five years of data per DOY to ensure statistical robustness. We spatially averaged GPP over the upstream area of each gauge. We present results for gauge Meisdorf as the primary study gauge, with results for all three gauges provided in the Supplements (Figure S8).

3 Results

The following sections present the evaluation of the coupled framework at the stand and catchment scale, the effect of parameter optimization on water balance partitioning, the sensitivity of the framework to key parameters, and the GPP–discharge relationship.

3.1 Evaluation of the vegetation component

FORMIND-mHM improved stand-scale agreement with eddy covariance observations at Hohes Holz relative to stand-alone FORMIND, for both ET and GPP, over the evaluation period 2015–2020 (Figure 3). For ET, FORMIND-mHM improved the agreement of the simulations with observations ($R^2 = 0.702$) relative to FORMIND ($R^2 = 0.551$), and the coupled framework produced slightly lower ET estimates during the vegetation period (Figure 3a). We found a similar improvement for GPP ($R^2 = 0.793$ vs. 0.614), with FORMIND-mHM producing lower GPP estimates in spring and early summer, which tend to be higher in stand-alone FORMIND in the absence of coupled soil moisture constraints (Figure 3b).

3.2 Evaluation of hydrologic component

To evaluate FORMIND-mHM at the catchment scale, we analysed the hydrological fluxes, partitioning, and discharge generation using mHM and the coupled model framework. Comparing actual evapotranspiration (AET) and soil saturation averaged over all forested cells with at least 70 % forest cover revealed similar hydrological dynamics in both optimized configurations. The coupled framework produced slightly higher AET (Figure 4a) and lower soil saturation during summer months (Figure 4b).

At gauge Meisdorf, the coupled framework achieved a KGE of 0.85 compared to 0.91 for stand-alone mHM, with closely matching correlation ($r = 0.90$ vs. 0.91), variability ($\alpha = 0.91$ vs. 1.00), and bias ($\beta = 0.94$ vs. 1.00) (Figure 4c). Both models tended to underestimate annual discharge across the simulation period (Figure 4d). Outside the vegetation period, FORMIND-

https://doi.org/10.5194/egusphere-2026-4918
Preprint. Discussion started: 31 August 2026

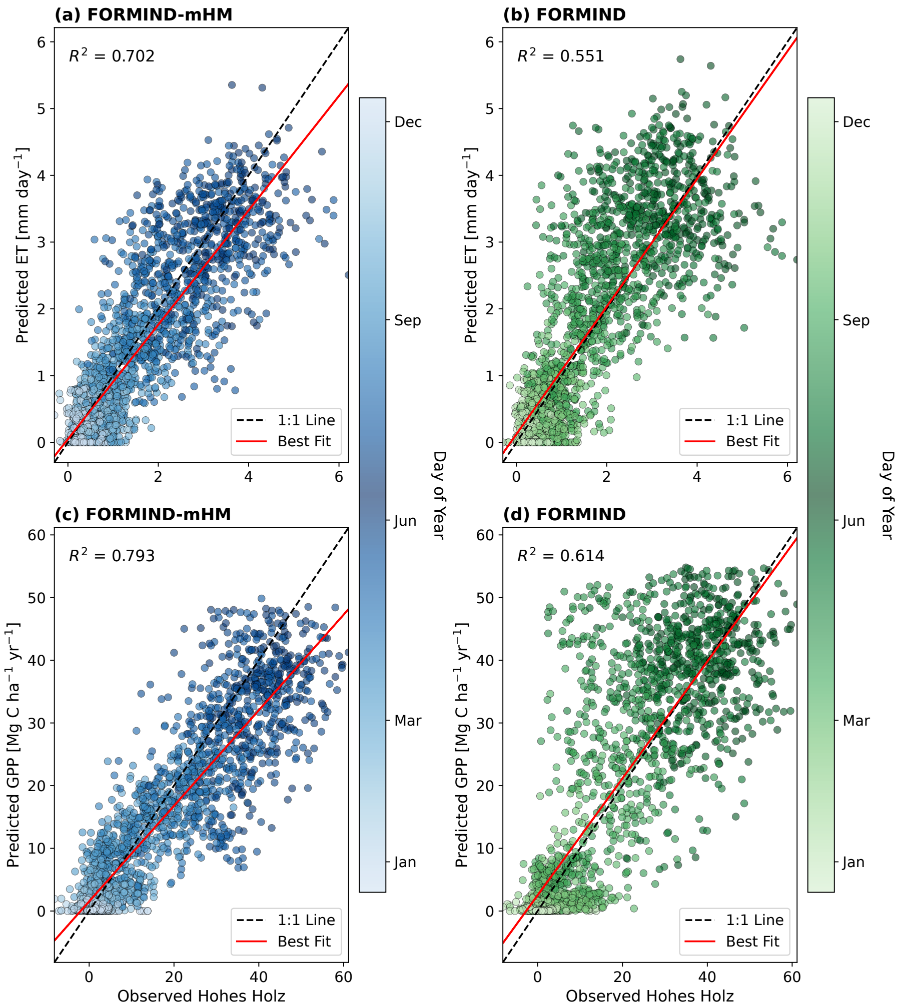

Figure 3. Scatter plots of **(a, b)** daily evapotranspiration (ET) and **(c, d)** gross primary production (GPP) for a temperate forest at Hohes Holz. We compared the coupled model framework (FORMIND-mHM) and stand-alone FORMIND against eddy covariance observations for the period 2015-2020. Observations are from an eddy covariance flux tower situated at the Hohes Holz. Both variables show improved agreement between FORMIND-mHM and observed fluxes compared to stand-alone FORMIND, as indicated by higher coefficients of determination (R^2).

mHM underestimated discharge, while showing closer agreement with observations during spring and summer (Figure 4e). Both models tended to underestimate discharge during low-flow periods, as indicated by the flow duration curve (Figure S2).

https://doi.org/10.5194/egusphere-2026-4918
Preprint. Discussion started: 31 August 2026

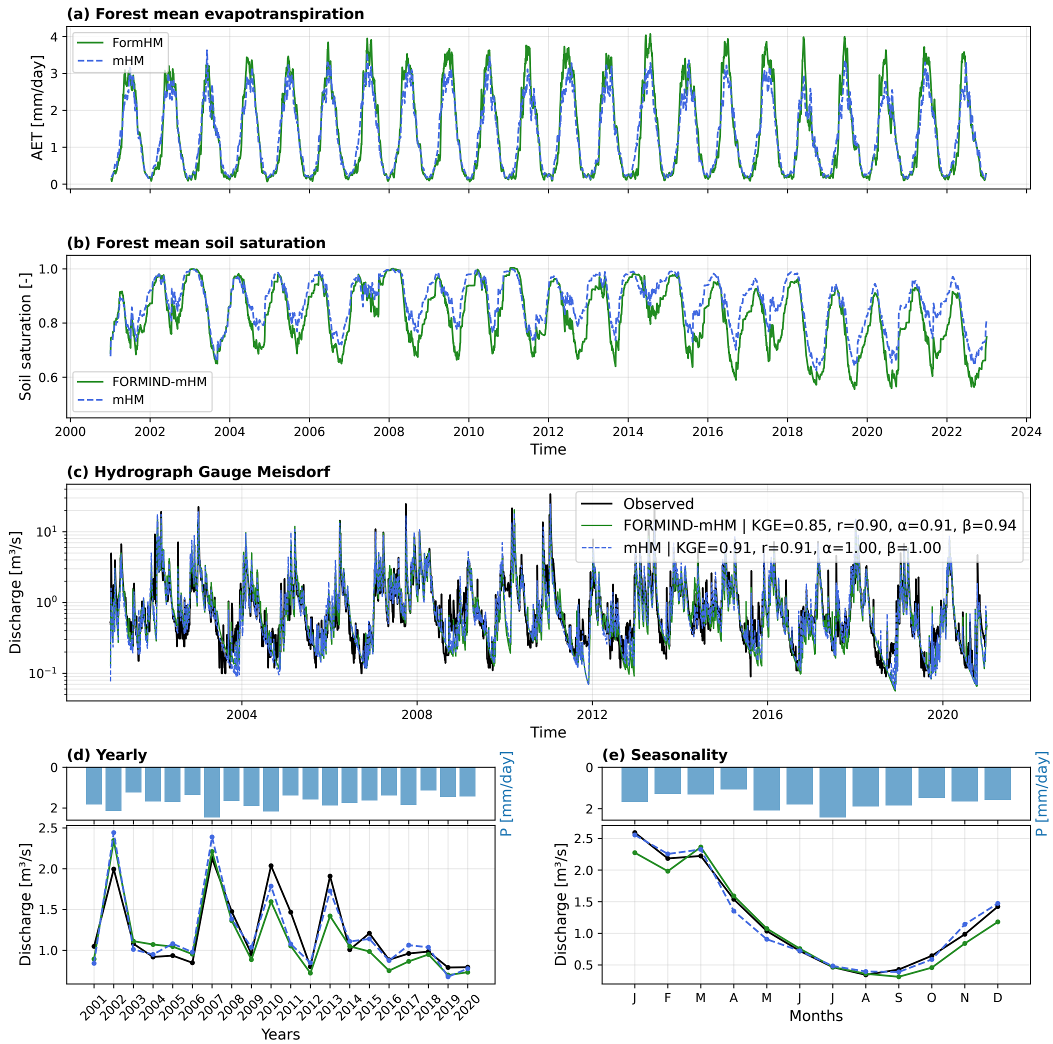

Figure 4. Comparison of FORMIND-mHM and stand-alone mHM for the Selke catchment with optimized soil parameters for gauge Meisdorf. **(a)** Forest mean actual evapotranspiration (AET) and **(b)** forest mean soil saturation for the period 2005-2023, showing close agreement between both model configurations. **(c)** Daily hydrograph at gauge Meisdorf on a logarithmic scale for the period 2001-2016, with Kling-Gupta efficiency (KGE), correlation coefficient (r), and bias components (α, β) for both configurations. **(d)** Annual mean discharge compared to observed values, with mean annual precipitation shown as bar chart. **(e)** Mean seasonal discharge climatology compared to observations, with mean monthly precipitation shown as bar chart.

3.3 Water balance partitioning and effect of parameter optimization

Table 1 summarizes water balance components and model performance for both optimized and non-optimized configurations of mHM and FORMIND-mHM for the more forested Meisdorf sub-catchment. Without any parameter optimization,

https://doi.org/10.5194/egusphere-2026-4918
Preprint. Discussion started: 31 August 2026

Table 1. Water balance components and model performance for the Selke catchment for the four model configurations: stand-alone mHM, initial coupling FORMIND-mHM, optimized mHM_{opt} for Meisdorf, and optimized coupling $\text{FORMIND-mHM}_{\text{opt}}$ for Meisdorf. Upper section: water balance components for the Meisdorf sub-catchment; lower section: performance metrics at the Meisdorf gauge.

	mHM	**FORMIND-mHM**	**mHM_{opt}**	**$\text{FORMIND-mHM}_{\text{opt}}$**
Sub-catchment: Gauge Meisdorf $\mathrm{mm\,yr^{-1}}$				
Transpiration	267.2	361.1	234.4	354.6
Evaporation	220.1	124.8	237.5	130.0
Exfiltration	179.7	180.8	194.1	182.1
Runoff	9.8	7.0	8.5	5.7
Δ Soil	1.0	0.7	3.2	2.2
Δ Snow	-0.6	-0.6	-0.6	-0.6
Total Flux	677.1	673.8	677.1	674.0
Precipitation	677.1	677.1	677.1	677.1
Closure Error	0.0	3.3	-0.0	3.2
Model performance – Meisdorf gauge [–]				
KGE	0.82	0.77	0.91	0.85
r	0.90	0.88	0.91	0.90
α	0.86	0.81	1.00	0.91
β	0.93	0.93	1.00	0.94

the initial coupling of FORMIND-mHM already achieved a KGE of 0.77 at gauge Meisdorf, demonstrating that the coupled framework produces hydrologically plausible results without requiring recalibration. Parameter optimization further improved model performance for both configurations: KGE increased to 0.85 for FORMIND-mHM and 0.91 for stand-alone mHM for the calibration period 2005–2015.

The two models diverged most strongly in the partitioning of evapotranspiration, shifting from canopy evaporation in mHM to transpiration in FORMIND-mHM. For the Meisdorf sub-catchment, FORMIND-mHM estimated 354.6 $\mathrm{mm\,yr^{-1}}$ to transpiration compared to 234.4 $\mathrm{mm\,yr^{-1}}$ in optimized mHM, while evaporation was correspondingly lower in FORMIND- mHM (130.0 $\mathrm{mm\,yr^{-1}}$ vs. 237.5 $\mathrm{mm\,yr^{-1}}$). This shift was consistent across both optimized and non-optimized configurations and was more pronounced in the Meisdorf sub-catchment than in the full catchment, reflecting the higher forest cover fraction of the former. Exfiltration and runoff remained broadly comparable between both model configurations in all experiments.

https://doi.org/10.5194/egusphere-2026-4918
Preprint. Discussion started: 31 August 2026

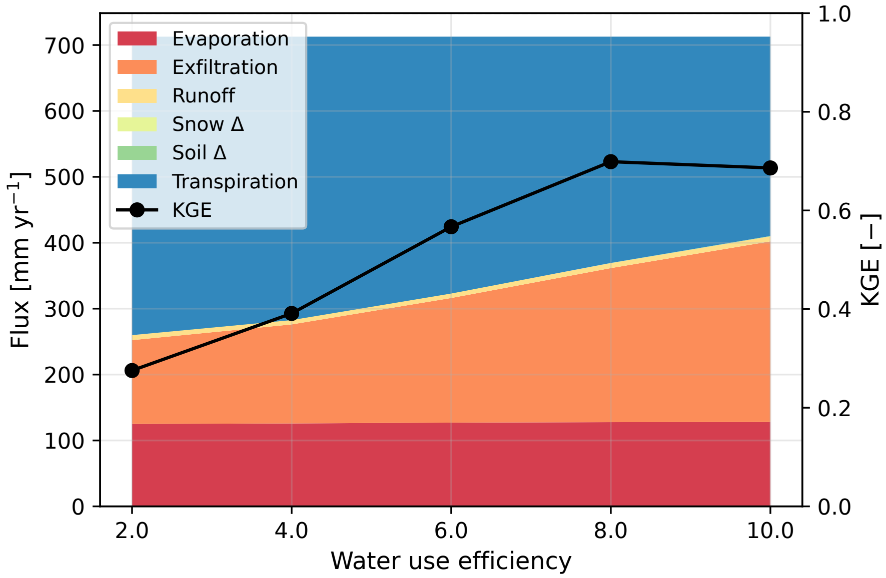

Figure 5. Sensitivity of water balance partitioning and discharge performance to water use efficiency of trees in FORMIND-mHM for a 10-year modelling period. Stacked bars show mean annual water flux components (transpiration, evaporation, exfiltration, surface runoff, and storage changes) as a function of WUE, with the Kling-Gupta efficiency (KGE) for discharge at gauge Meisdorf shown as a line (right axis).

3.4 Parameter sensitivity tests

To better understand the sensitivity of the coupled framework to key parameters and to identify which aspects of the model are most responsive to cross-domain constraint, we tested the response of FORMIND-mHM to variations in two parameters: WUE in FORMIND and the canopy interception constant in mHM. Increasing WUE in the forest simulation shifted water balance partitioning away from transpiration towards exfiltration and runoff. At gauge Meisdorf, this was accompanied by a steady increase in KGE with WUE, which peaked at WUE,=,8 before stabilizing (Figure 5). Across five WUE values, increasing WUE from 2 to 8 increased KGE from ≈ 0.3 to ≈ 0.7. In contrast, varying the canopy interception constant across four values in stand-alone mHM indicated little influence on model performance or water balance partitioning across the tested range (Figure S4).

3.5 GPP-discharge relationship

The seasonal relationship between simulated GPP and observed discharge at gauge Meisdorf revealed a pronounced anti-phase dynamic over the course of the year (Figure 6). GPP rose steeply from near zero in January to a peak of approximately $30\,\mathrm{Mg\,C\,ha^{-1}\,yr^{-1}}$ in June, while discharge followed the opposite trajectory, declining from winter highs of around 2–3 $\mathrm{m^3\,s^{-1}}$ to summer minima below 0.5 $\mathrm{m^3\,s^{-1}}$(Figure 6b). This anti-phase pattern was also reflected in the interannual correla-

https://doi.org/10.5194/egusphere-2026-4918
Preprint. Discussion started: 31 August 2026

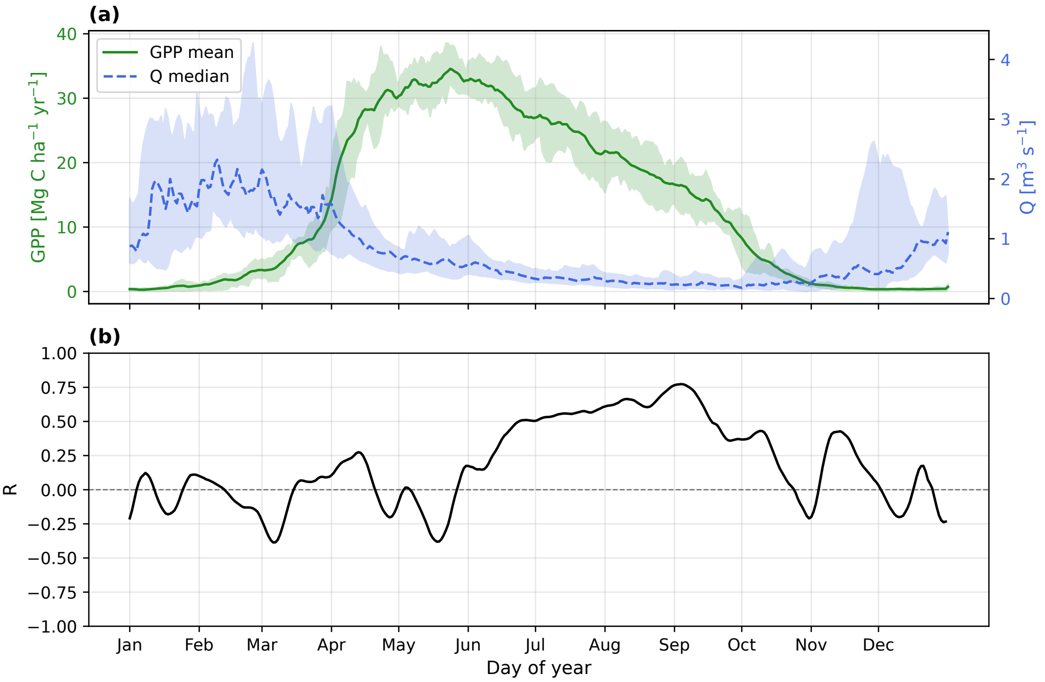

Figure 6. Seasonal relationship between simulated gross primary production (GPP) and observed discharge (Q) at gauge Meisdorf. **(a)** Mean seasonal cycles of simulated GPP (green, left axis) and observed discharge (blue, right axis), with shaded areas indicating the interquartile range across years. **(b)** Inter- annual correlation coefficient (R) between GPP and Q as a function of day of year, calculated using a 7-day smoothing window, a lag of 15 days, and a day- of-year window of ±7 days.

tion coefficient R, which describes, for each day of year, how strongly annual anomalies in GPP covary with annual anomalies in discharge across years. R shifted from weakly negative in January and February to strongly negative in March and April (R ≈ -0.5), before turning positive through summer and peaking above 0.5 between July and September (Figure 6a). The transition from negative to positive R in late April coincided with the onset of the growing season, when increasing vegetation water demand suppresses discharge. This seasonal pattern was consistent across all three gauging stations within the Selke catchment (Figure S8). The wide uncertainty band in discharge throughout winter and spring reflects high inter-annual variability in snowmelt and precipitation timing, in contrast to the comparatively consistent GPP trajectory across years.

4 Discussion

In this study, we coupled the individual-based forest gap model FORMIND with the mesoscale hydrological model mHM to investigate how the spatial and process-level differences between the two models can be reconciled within a coupled framework, how the coupling affects hydrological flux partitioning, and whether it improves the representation of key hydrologic processes. Further, we tested the possibility of cross-domain parameter inference and if catchment-scale river discharge carries

https://doi.org/10.5194/egusphere-2026-4918
Preprint. Discussion started: 31 August 2026

information about stand-scale GPP of forests. The coupled framework achieved performance comparable to stand-alone mHM for key hydrological variables while simultaneously improving ET and GPP estimates relative to stand-alone FORMIND, suggesting that the integration of dynamic vegetation adds relevant information without sacrificing hydrological predictive skill. The most notable structural difference between the two model configurations was a shift from evaporation-dominated to transpiration-dominated ET partitioning, which has direct consequences for soil moisture dynamics and the representation of vegetation water stress in forested catchments. Finally, the seasonal GPP–discharge relationship and the cross-domain parameter inference demonstrated that coupled modelling frameworks open analytical pathways that are inaccessible to either stand-alone model.

The coupled framework presented here differs from existing vegetation-hydrology coupling approaches in its combination of process detail and temporal resolution. While several such frameworks have been developed, they vary considerably in their representation of forest dynamics and hydrological processes. Here, we explicitly coupled stand-scale vegetation dynamics with catchment-scale hydrological processes. One comparable approach is FORHYCS, a distributed ecohydrological model, developed by Speich et al. (2020), who coupled the forest model TreeMig (Lischke et al., 2006) with the hydrological model PREVAH (Gurtz et al., 1999) and applied it to an alpine catchment in Switzerland. The coupling case study demonstrated that dynamic vegetation representation substantially affects simulated streamflow under climate change. The coupling is based on the assumption that the current-year water balance has negligible effects on forest structure, not considering within-year drought responses that are central to the research questions addressed here. In comparison, FORMIND-mHM addressed this limitation as the daily data exchange between model components captures seasonal vegetation–water feedbacks that are lost in annual coupling schemes.

Jia et al. (2026) coupled LPJ-GUESS (Smith et al., 2001, 2014) with the three-dimensional subsurface flow model ParFlow (Ashby and Falgout, 1996; Jones and Woodward, 2001; Kollet and Maxwell, 2006) and applied the framework (PF-LPJG) across the Danube River Basin. The coupled model substantially improved streamflow and surface soil moisture simulations relative to stand-alone LPJ-GUESS without requiring parameter calibration. Several conceptual differences distinguish PF-LPJG from the FORMIND-mHM framework presented here. First, LPJ-GUESS represents vegetation as age cohorts, meaning that fine-scale structural heterogeneity in canopy composition and competition is not resolved. Second, the two frameworks differ in the variables exchanged and the coupling strategy employed. In PF-LPJG, LPJ-GUESS provides net atmospheric water input (P-ET) as an upper boundary condition to ParFlow, which in turn overwrites the internal soil moisture states of LPJ-GUESS with updated soil moisture and surface/subsurface runoff fields, replacing LPJ-GUESS's native soil module. In FORMIND-mHM, by contrast, the exchange is centred on the vegetation–water interface. The soil component mediates between the two models while both retain their native structure, making the vegetation–carbon feedback explicit in the coupling interface. Third, while the inter-model data exchange operates at a daily timestep in both frameworks, PF-LPJG disaggregates daily P-ET values into hourly inputs for ParFlow's internal calculation, capturing sub-daily soil moisture dynamics at the cost of substantial modifications to the LPJ-GUESS source code, limiting the transferability of the approach to other model combinations. Here, using the FINAM framework avoids invasive modifications to the source code of either stand-alone model

https://doi.org/10.5194/egusphere-2026-4918
Preprint. Discussion started: 31 August 2026

and retains the vegetation–carbon feedback as an explicit part of the coupling interface, while remaining transferable to other model combinations.

4.1 Implications of coupled vegetation–hydrology modelling

The coupled framework yielded values of evapotranspiration partitioning which are more in line with observational data. Transpiration in forests typically dominates ET, with transpiration fractions (E_t/ET) ranging from 0.54 to 0.90 depending on forest type (Wei et al., 2017; Hassan et al., 2026), yet transpiration in stand-alone mHM accounts for only roughly half of total evapotranspiration in forested areas. The coupled framework produced a transpiration fraction of 0.73 for forested areas, substantially closer to observed ranges, suggesting that the dynamic vegetation representation provides a more process-consistent partitioning of evapotranspiration than the static LAI parametrisation used in stand-alone mHM. This shift had direct consequences for simulated soil moisture dynamics, with the coupled framework producing lower summer soil moisture levels than stand-alone mHM, a difference that remains plausible but could not be directly validated against observations in the absence of corresponding field data. The practical relevance of this difference is greatest in heterogeneous landscapes where forest cover varies substantially across sub-catchments, as the coupled framework responded to spatial variation in forest structure in a way that stand-alone mHM cannot.

Within the coupled model framework the soil became more prone to soil moisture depletion than compared to stand-alone FORMIND. The multi-layer soil representation in the coupled framework refined the simulation of vegetation water stress relative to stand-alone FORMIND, and directly contributed to the improved GPP agreement observed at Hohes Holz. The single soil layer used in stand-alone FORMIND implies that water stress is governed by the mean moisture of the entire rooting zone, which can mask depletion in the top soil. In the coupled framework, water uptake per layer was limited by the relative root fraction and the remaining evapotranspiration potential, meaning that low soil moisture in upper layers could not be compensated by increased uptake from deeper layers. This made the model more sensitive to soil moisture depletion in early summer, suppressing GPP earlier in the vegetation season and reducing the overestimation shown by stand-alone FORMIND during this period. This is consistent with the higher R^2 values observed for FORMIND-mHM relative to stand-alone FORMIND (Figure 3).

Besides improving process representation, the coupled model framework enables the investigation of cross-domain relationships. Kim et al. (2018) demonstrated in an experiment with a temperate deciduous forest receiving approximately twice the annual precipitation of the Selke catchment that increased GPP leads to a significant reduction in annual catchment discharge. Here, we inverted this perspective to examine whether river discharge itself carries exploitable information about GPP. The seasonal reversal from a negative to a positive GPP–discharge relationship around peak GPP reflected the onset of water limitation: as transpiration increased with rising GPP, soil moisture was progressively depleted, and the resulting reduction in available water constrained both GPP and discharge generation, producing a positive correlation. Outside of late summer, the signal remained comparatively weak for most of the rest of the year (Figure 4b), when both variables were governed by a wider range of environmental drivers not captured by this bivariate signal. These results illustrate a broader point: by coupling vegetation

https://doi.org/10.5194/egusphere-2026-4918
Preprint. Discussion started: 31 August 2026

and hydrological domains within a single framework, statistical relationships between state variables of different ecosystem compartments become directly testable, opening analytical pathways that are inaccessible to either stand-alone model.

Further, the coupled framework offers now opportunities for cross-domain parameter inference. The sensitivity of discharge performance to WUE demonstrated that hydrological observations could be used to constrain forest ecophysiological parameters that are otherwise difficult to determine at the stand scale. While WUE can be estimated at the ecosystem level as the ratio of GPP to evapotranspiration, it exhibits substantial variability across ecosystem types, years, and climatic conditions (Beer et al., 2009), reflecting the complexity of the underlying biochemical processes that regulate the carbon-water trade-off in plants and their stomata (Medlyn et al., 2011). This makes the selection of a representative value for a heterogeneous catchment a non-trivial task without observational constraints. The results presented here suggest that discharge observations at gauging stations, which are far more widely available than eddy covariance measurements, could provide a practical pathway for constraining WUE at the stand scale.

4.2 Trade-offs, applicability, and technical considerations

The described advantages of a coupled model system came at the cost of increased model complexity. Rather than parametrising a single model, the coupled framework required the parametrisation of both FORMIND and mHM, each with their own parameter sets and calibration requirements. Furthermore, the coupled framework was substantially slower to execute than stand-alone mHM, as it combined the computational cost of running FORMIND, which is inherently more computationally expensive than mHM due to its individual-based simulation of tree dynamics, with the additional overhead of the snow and soil modules that needed to be implemented to bridge the differing spatial scales of the two models. This had direct implications for model calibration, as a full calibration of the coupled system requires a large number of model runs, making automated parameter optimisation approaches computationally difficult without further performance improvements of the coupled model. This issue could be mitigated by parallelising the execution of FORMIND in the different forest cells. Nonetheless, for applications where full parameter optimisation is essential, models that integrate vegetation dynamics internally, such as LPJ-GUESS (Smith et al., 2001), may offer a more computationally tractable alternative, notably at the cost of reduced process detail at the stand scale.

These advantages and trade-offs raise the question when coupling is worthwhile, and suggest that the value of coupling depends strongly on the research question and application context. The coupled framework is particularly suited to studies where vegetation–water feedbacks are central to the research question. This includes long-term projections under environmental change, where static vegetation representations cannot capture forest mortality, succession, or structural reorganisation, and catchments with spatially heterogeneous forest cover, where the dynamic vegetation representation provides more robust parameter transferability than a statically parametrised model. The insensitivity of stand-alone mHM to changes in the canopy interception parameter illustrates this point further: the static vegetation representation could not translate structural differences in forest canopy into meaningful hydrological responses. Besides these long-term studies, coupling may be particularly worthwhile for studies focusing on the forest stand scale, where the hydrological consequences of structural changes in forest composition could in principle be resolved directly.

https://doi.org/10.5194/egusphere-2026-4918
Preprint. Discussion started: 31 August 2026

Conversely, the added complexity of coupling may not be justified when discharge prediction is the primary objective, as stand-alone mHM achieved more accurate results in this regard and was computationally more efficient. Additionally, the coupled framework requires a forest initialisation workflow for FORMIND, which may make its application challenging in data-sparse regions. Similarly, coupling adds most value to forest modelling if water limitation is a central driver of forest dynamics, for instance in drought scenarios or under projected increases in evaporative demand. In cases where water availability is not a primary constraint on forest growth, stand-alone FORMIND may provide equally adequate representations of forest dynamics at lower computational cost and effort.

The FINAM model coupling framework (Müller et al., 2025) enables a component-based architecture with flexible data exchange between models, allowing each model to retain its native structure while communicating through well-defined interfaces. The additional complexity of the coupled system arises from two structural requirements rather than from limitations of FINAM itself: providing each FORMIND patch with its own soil moisture storage required an independent soil moisture component operating at patch scale, and the sequential calculation order of mHM then necessitated extracting the snow module as a separate component to maintain the correct process sequence.

We selected FINAM (Müller et al., 2025) over alternative coupling frameworks such as BMI (Peckham et al., 2013; Hutton et al., 2020) and OpenMI (Moore and Tindall, 2005; Gregersen et al., 2007; Harpham et al., 2019) for its Python-native implementation, built-in infrastructure for scheduling and component management, and its ability to integrate new Python modules directly into the coupling pipeline. These features were essential for implementing the snow and soil modules as independent components.

5 Conclusions

In this study, we coupled the forest model FORMIND with the hydrological model mHM to examine the feasibility of integrating dynamic vegetation into a distributed hydrological model and to assess how this integration affects hydrological partitioning. We showed that an initial, non-optimized coupling of both models already achieved good model performance, with further improvements gained through parameter optimization. The integration of dynamic vegetation had a significant effect on hydrological partitioning, shifting evapotranspiration from evaporation-dominated to transpiration-dominated, with direct consequences for soil moisture dynamics. The coupled framework further achieved a catchment-wide closed water balance, a fundamental prerequisite for credible long-term simulations of ecohydrological dynamics. Additionally, we demonstrated that catchment-scale discharge carries exploitable information about stand-scale GPP, with a seasonal relationship that emerged from the shared dependence of both variables on soil moisture availability.

Among existing coupled frameworks, FORMIND-mHM is one of the few that combines individual-based forest modelling with mesoscale hydrology, explicitly resolving the growth, mortality, and competition of individual trees while simultaneously representing catchment-scale water fluxes. This makes it particularly well suited for questions at the forest management scale, where the hydrological consequences of specific management decisions can be directly simulated. These are questions that

https://doi.org/10.5194/egusphere-2026-4918
Preprint. Discussion started: 31 August 2026

coarser vegetation representations, such as those used in land surface models or population-based forest models, cannot address at the required level of process detail.

These results demonstrate that explicit coupling of vegetation and hydrological models offers both a more process-consistent representation of water–vegetation feedbacks and new opportunities for cross-domain model evaluation. As pressures on forest and water resources continue to intensify under environmental changes, frameworks such as FORMIND-mHM provide a pathway towards more integrated predictions of ecohydrological dynamics across ecosystem boundaries.

Code and data availability. The mHM code is available on Zenodo at https://doi.org/10.5281/zenodo.21670439 (Samaniego et al., 2026). The Formind-mHM code is available on Zenodo at https://doi.org/10.5281/zenodo.21904998 (Bruns et al., 2026). The sources of the corresponding datasets for model setup and forcings are out lined in detail in Sect. 2

Author contributions. Niklas Bruns: Methodology, Software, Validation, Formal analysis, Investigation, Writing - Original Draft, Visualization. Andreas Huth: Writing - Review & Editing, Supervision. Stephan Thober: Conceptualization, Methodology, Writing - Review & Editing, Supervision. Samuel M. Fischer: Conceptualization, Methodology, Writing - Review & Editing, Supervision.

Competing interests. The contact author has declared that none of the authors has any competing interests.

Acknowledgements. The authors would like to thank the FINAM developer team for their technical support, as well as the members of the LISA PhD College and consortium, and the FORMIND working group, for valuable discussions and feedback. The authors acknowledge the usage of AI tools (Claude Code) for code review.

https://doi.org/10.5194/egusphere-2026-4918
Preprint. Discussion started: 31 August 2026

References

Allen, C. D., Macalady, A. K., Chenchouni, H., Bachelet, D., McDowell, N., Vennetier, M., Kitzberger, T., Rigling, A., Breshears, D. D., Hogg, E. H. T., Gonzalez, P., Fensham, R., Zhang, Z., Castro, J., Demidova, N., Lim, J.-H., Allard, G., Running, S. W., Semerci, A., and Cobb, N.: A global overview of drought and heat-induced tree mortality reveals emerging climate change risks for forests, Forest Ecology and Management, 259, 660–684, https://doi.org/10.1016/j.foreco.2009.09.001, 2010.

Andréassian, V.: Waters and forests: from historical controversy to scientific debate, Journal of Hydrology, 291, 1–27, https://doi.org/10.1016/j.jhydrol.2003.12.015, 2004.

Ashby, S. F. and Falgout, R. D.: A Parallel Multigrid Preconditioned Conjugate Gradient Algorithm for Groundwater Flow Simulations, Nuclear Science and Engineering, 124, 145–159, https://doi.org/10.13182/NSE96-A24230, _eprint: https://doi.org/10.13182/NSE96-A24230, 1996.

Bauer, L., Knapp, N., and Fischer, R.: Mapping Amazon Forest Productivity by Fusing GEDI Lidar Waveforms with an Individual-Based Forest Model, Remote Sensing, 13, 4540, https://doi.org/10.3390/rs13224540, 2021.

Bauer, L., Huth, A., Bogdanowski, A., Müller, M., and Fischer, R.: Edge Effects in Amazon Forests: Integrating Remote Sensing and Modelling to Assess Changes in Biomass and Productivity, Remote Sensing, 16, 501, https://doi.org/10.3390/rs16030501, number: 3, 2024.

Beaulieu, E., Lucas, Y., Viville, D., Chabaux, F., Ackerer, P., Goddéris, Y., and Pierret, M.-C.: Hydrological and vegetation response to climate change in a forested mountainous catchment, Modeling Earth Systems and Environment, 2, 1–15, https://doi.org/10.1007/s40808-016-0244-1, 2016.

Beer, C., Ciais, P., Reichstein, M., Baldocchi, D., Law, B. E., Papale, D., Soussana, J., Ammann, C., Buchmann, N., Frank, D., Gianelle, D., Janssens, I. A., Knohl, A., Köstner, B., Moors, E., Roupsard, O., Verbeeck, H., Vesala, T., Williams, C. A., and Wohlfahrt, G.: Temporal and among-site variability of inherent water use efficiency at the ecosystem level, Global Biogeochemical Cycles, 23, 2008GB003 233, https://doi.org/10.1029/2008GB003233, 2009.

Boeing, F., Rakovec, O., Kumar, R., Samaniego, L., Schrön, M., Hildebrandt, A., Rebmann, C., Thober, S., Müller, S., Zacharias, S., Bogena, H., Schneider, K., Kiese, R., Attinger, S., and Marx, A.: High-resolution drought simulations and comparison to soil moisture observations in Germany, Hydrology and Earth System Sciences, 26, 5137–5161, https://doi.org/10.5194/hess-26-5137-2022, 2022.

Boeing, F., Attinger, S., Wagener, T., Rakovec, O., Samaniego, L., Thober, S., Schlaak, J., Müller, S., Teichmann, C., Kumar, R., and Marx, A.: Spatially and Seasonally Differentiated Response of Soil Moisture Droughts to Climate Change in Germany, Earth's Future, 13, e2024EF005 495, https://doi.org/10.1029/2024EF005495, _eprint: https://agupubs.onlinelibrary.wiley.com/doi/pdf/10.1029/2024EF005495, 2025.

Bohn, F. J., Frank, K., and Huth, A.: Of climate and its resulting tree growth: Simulating the productivity of temperate forests, Ecological Modelling, 278, 9–17, https://doi.org/10.1016/j.ecolmodel.2014.01.021, 2014.

Bruns, N., Huth, A., Thober, S., and Fischer, S.: Combining an individual-based dynamic vegetation model with a distributive hydrologic model to improve coupled water-carbon modelling, https://doi.org/10.5281/zenodo.21904998, 2026.

Bugmann, H. and Seidl, R.: The evolution, complexity and diversity of models of long-term forest dynamics, Journal of Ecology, 110, 2288–2307, https://doi.org/10.1111/1365-2745.13989, _eprint: https://besjournals.onlinelibrary.wiley.com/doi/pdf/10.1111/1365-2745.13989, 2022.

Choat, B., Jansen, S., Brodribb, T. J., Cochard, H., Delzon, S., Bhaskar, R., Bucci, S. J., Feild, T. S., Gleason, S. M., Hacke, U. G., Jacobsen, A. L., Lens, F., Maherali, H., Martínez-Vilalta, J., Mayr, S., Mencuccini, M., Mitchell, P. J., Nardini, A., Pittermann, J., Pratt, R. B., Sperry, J. S., Westoby, M., Wright, I. J., and Zanne, A. E.: Global convergence in the vulnerability of forests to drought, Nature, 491, 752–755, https://doi.org/10.1038/nature11688, 2012.

Drollinger, S., Dietze, M., Seidel, D., Schwindt, D., Birk, J. J., and Sauer, D.: Recent changes in rainfall patterns alter precipitation partitioning in European beech forest, Environmental Research Communications, 7, 031 004, https://doi.org/10.1088/2515-7620/adbba4, 2025.

Díaz-Yáñez, O., Käber, Y., Anders, T., Bohn, F., Braziunas, K. H., Brůna, J., Fischer, R., Fischer, S. M., Hetzer, J., Hickler, T., Hochauer, C., Lexer, M. J., Lischke, H., Mairota, P., Merganič, J., Merganičová, K., Mette, T., Mina, M., Morin, X., Nieberg, M., Rammer, W., Reyer, C. P. O., Scheiter, S., Scherrer, D., and Bugmann, H.: Tree regeneration in models of forest dynamics: A key priority for further research, Ecosphere, 15, e4807, https://doi.org/10.1002/ecs2.4807, 2024.

Ellison, D., Morris, C. E., Locatelli, B., Sheil, D., Cohen, J., Murdiyarso, D., Gutierrez, V., Noordwijk, M. v., Creed, I. F., Pokorny, J., Gaveau, D., Spracklen, D. V., Tobella, A. B., Ilstedt, U., Teuling, A. J., Gebrehiwot, S. G., Sands, D. C., Muys, B., Verbist, B., Springgay, E., Sugandi, Y., and Sullivan, C. A.: Trees, forests and water: Cool insights for a hot world, Global Environmental Change, 43, 51–61, https://doi.org/10.1016/j.gloenvcha.2017.01.002, 2017.

Fatichi, S., Pappas, C., and Ivanov, V. Y.: Modeling plant–water interactions: an ecohydrological overview from the cell to the global scale, WIREs Water, 3, 327–368, https://doi.org/10.1002/wat2.1125, _eprint: https://wires.onlinelibrary.wiley.com/doi/pdf/10.1002/wat2.1125, 2016a.

Fatichi, S., Vivoni, E. R., Ogden, F. L., Ivanov, V. Y., Mirus, B., Gochis, D., Downer, C. W., Camporese, M., Davison, J. H., Ebel, B., Jones, N., Kim, J., Mascaro, G., Niswonger, R., Restrepo, P., Rigon, R., Shen, C., Sulis, M., and Tarboton, D.: An overview of current applications, challenges, and future trends in distributed process-based models in hydrology, Journal of Hydrology, 537, 45–60, https://doi.org/10.1016/j.jhydrol.2016.03.026, 2016b.

Felton, A. J., Fisher, J. B., Hufkens, K., Purdy, A. J., Spawn-Lee, S. A., Duloisy, L. F., and Goldsmith, G. R.: Global estimates of the storage and transit time of water through vegetation, Nature Water, 3, 59–69, https://doi.org/10.1038/s44221-024-00365-9, 2025.

Fischer, R., Bohn, F., Dantas De Paula, M., Dislich, C., Groeneveld, J., Gutiérrez, A. G., Kazmierczak, M., Knapp, N., Lehmann, S., Paulick, S., Pütz, S., Rödig, E., Taubert, F., Köhler, P., and Huth, A.: Lessons learned from applying a forest gap model to understand ecosystem and carbon dynamics of complex tropical forests, Ecological Modelling, 326, 124–133, https://doi.org/10.1016/j.ecolmodel.2015.11.018, 2016.

Fischer, R., Anders, T., Bugmann, H., Djahangard, M., Dreßler, G., Hetzer, J., Hickler, T., Hiltner, U., Marano, G., Sperlich, D., Yousefpour, R., and Knapp, N.: Perspectives for forest modeling to improve the representation of drought-related tree mortality, Journal für Kulturpflanzen, 77, 50–69, https://doi.org/10.5073/JfK.2025.02.05, number: 02, 2025.

Fischer, S. M., Fischer, R., and Huth, A.: Assessing forest biomass and productivity with data-driven vegetation indices: insights from 900 000 simulated forest stands, Biogeosciences, 23, 4927–4942, https://doi.org/10.5194/bg-23-4927-2026, 2026.

Granier, A., Bréda, N., Biron, P., and Villette, S.: A lumped water balance model to evaluate duration and intensity of drought constraints in forest stands, Ecological Modelling, 116, 269–283, https://doi.org/10.1016/S0304-3800(98)00205-1, 1999.

Gregersen, J. B., Gijsbers, P. J. A., and Westen, S. J. P.: OpenMI: Open modelling interface, Journal of Hydroinformatics, 9, 175–191, https://doi.org/10.2166/hydro.2007.023, 2007.

Gurtz, J., Baltensweiler, A., and Lang, H.: Spatially distributed hydrotope-based modelling of evapotranspiration and runoff in mountainous basins, Hydrological Processes, 13, 2751–2768, https://doi.org/10.1002/(SICI)1099-

https://doi.org/10.5194/egusphere-2026-4918
Preprint. Discussion started: 31 August 2026

1085(19991215)13:17<2751::AID-HYP897>3.0.CO;2-O, _eprint: https://onlinelibrary.wiley.com/doi/pdf/10.1002/%28SICI%291099-1085%2819991215%2913%3A17%3C2751%3A%3AAID-HYP897%3E3.0.CO%3B2-O, 1999.

Harpham, Q. K., Hughes, A., and Moore, R. V.: Introductory overview: The OpenMI 2.0 standard for integrating numerical models, Environmental Modelling & Software, 122, 104 549, https://doi.org/10.1016/j.envsoft.2019.104549, 2019.

Hassan, A., Prentice, I. C., and Liang, X.: Insights into evapotranspiration partitioning based on hydrological observations using the generalized proportionality hypothesis, Hydrology and Earth System Sciences, 30, 317–341, https://doi.org/10.5194/hess-30-317-2026, 2026.

Holtmann, A., Huth, A., Pohl, F., Rebmann, C., and Fischer, R.: Carbon Sequestration in Mixed Deciduous Forests: The Influence of Tree Size and Species Composition Derived from Model Experiments, Forests, 12, 726, https://doi.org/10.3390/f12060726, number: 6, 2021.

Hutton, E. W. h., Piper, M. D., and Tucker, G. E.: The Basic Model Interface 2.0: A standard interface for coupling numerical models in the geosciences, Journal of Open Source Software, 5, 2317, https://doi.org/10.21105/joss.02317, 2020.

Jasechko, S., Sharp, Z. D., Gibson, J. J., Birks, S. J., Yi, Y., and Fawcett, P. J.: Terrestrial water fluxes dominated by transpiration, Nature, 496, 347–350, https://doi.org/10.1038/nature11983, 2013.

Jia, Z., Chen, S., Fu, Y. H., Martín Belda, D., Wårlind, D., Olin, S., Xu, C., and Tang, J.: Advancing ecohydrological modelling: coupling LPJ-GUESS with ParFlow for integrated vegetation and surface-subsurface hydrology simulations, Geoscientific Model Development, 19, 1727–1747, https://doi.org/10.5194/gmd-19-1727-2026, 2026.

Jones, J. E. and Woodward, C. S.: Newton–Krylov-multigrid solvers for large-scale, highly heterogeneous, variably saturated flow problems, Advances in Water Resources, 24, 763–774, https://doi.org/10.1016/S0309-1708(00)00075-0, 2001.

Kim, J. H., Hwang, T., Yang, Y., Schaaf, C. L., Boose, E., and Munger, J. W.: Warming-Induced Earlier Greenup Leads to Reduced Stream Discharge in a Temperate Mixed Forest Catchment, Journal of Geophysical Research: Biogeosciences, 123, 1960–1975, https://doi.org/10.1029/2018JG004438, _eprint: https://agupubs.onlinelibrary.wiley.com/doi/pdf/10.1029/2018JG004438, 2018.

Kollet, S. J. and Maxwell, R. M.: Integrated surface–groundwater flow modeling: A free-surface overland flow boundary condition in a parallel groundwater flow model, Advances in Water Resources, 29, 945–958, https://doi.org/10.1016/j.advwatres.2005.08.006, 2006.

Kordrostami, F., Ustin, S. L., Koltunov, A., Tigabu, T. B., and Dahlke, H. E.: What is the current state and potential for hydrologic models to simulate vegetation dynamically?, Journal of Hydrology, 660, 133 401, https://doi.org/10.1016/j.jhydrol.2025.133401, 2025.

Kumar, R., Samaniego, L., and Attinger, S.: Implications of distributed hydrologic model parameterization on water fluxes at multiple scales and locations, Water Resources Research, 49, 360–379, https://doi.org/10.1029/2012WR012195, 2013.

Köhler, P. and Huth, A.: The effects of tree species grouping in tropical rainforest modelling: Simulations with the individual-based model Formind, Ecological Modelling, 109, 301–321, https://doi.org/10.1016/S0304-3800(98)00066-0, 1998.

Liang, X., Lettennmaier, D. P., Wood, E. F., and Burges, S. J.: A simple hydrologically based model of land surface water and energy fluxes for general circulation models, Journal of Geophysical Research, 99, 14,415–14,428, https://doi.org/10.1029/94JD00483, aDS Bibcode: 1994JGR....9914415L, 1994.

Lischke, H., Zimmermann, N. E., Bolliger, J., Rickebusch, S., and Löffler, T. J.: TreeMig: A forest-landscape model for simulating spatio-temporal patterns from stand to landscape scale, Ecological Modelling, 199, 409–420, https://doi.org/10.1016/j.ecolmodel.2005.11.046, 2006.

Maidment, D. R., ed.: Handbook of hydrology, McGraw-Hill, New York, 6. [print.] edn., ISBN 978-0-07-039732-3, 1995.

Medlyn, B. E., Duursma, R. A., Eamus, D., Ellsworth, D. S., Prentice, I. C., Barton, C. V. M., Crous, K. Y., De Angelis, P., Freeman, M., and Wingate, L.: Reconciling the optimal and empirical approaches to modelling stomatal conductance, Global Change Biology, 17, 2134–2144, https://doi.org/10.1111/j.1365-2486.2010.02375.x, _eprint: https://onlinelibrary.wiley.com/doi/pdf/10.1111/j.1365-2486.2010.02375.x, 2011.

Moore, R. V. and Tindall, C. I.: An overview of the open modelling interface and environment (the OpenMI), Environmental Science & Policy, 8, 279–286, https://doi.org/10.1016/j.envsci.2005.03.009, 2005.

Müller, S., Lange, M., Fischer, T., König, S., Kelbling, M., Leal Rojas, J. J., and Thober, S.: FINAM is not a model (v1.0): a new Python-based model coupling framework, Geoscientific Model Development, 18, 4483–4498, https://doi.org/10.5194/gmd-18-4483-2025, 2025.

Peckham, S. D., Hutton, E. W. H., and Norris, B.: A component-based approach to integrated modeling in the geosciences: The design of CSDMS, Computers & Geosciences, 53, 3–12, https://doi.org/10.1016/j.cageo.2012.04.002, 2013.

Pohl, F., Werban, U., Kumar, R., Hildebrandt, A., and Rebmann, C.: Observational evidence of legacy effects of the 2018 drought on a mixed deciduous forest in Germany, Scientific Reports, 13, 10 863, https://doi.org/10.1038/s41598-023-38087-9, 2023.

Rödig, E., Cuntz, M., Heinke, J., Rammig, A., and Huth, A.: Spatial heterogeneity of biomass and forest structure of the Amazon rain forest: Linking remote sensing, forest modelling and field inventory, Global Ecology and Biogeography, 26, 1292–1302, https://doi.org/10.1111/geb.12639, 2017a.

Rödig, E., Huth, A., Bohn, F., Rebmann, C., and Cuntz, M.: Estimating the carbon fluxes of forests with an individual-based forest model, Forest Ecosystems, 4, 4, https://doi.org/10.1186/s40663-017-0091-1, 2017b.

Rödig, E., Knapp, N., Fischer, R., Bohn, F. J., Dubayah, R., Tang, H., and Huth, A.: From small-scale forest structure to Amazon-wide carbon estimates, Nature Communications, 10, 5088, https://doi.org/10.1038/s41467-019-13063-y, 2019.

Sahu, M. K., Shwetha, H. R., and Dwarakish, G. S.: State-of-the-art hydrological models and application of the HEC-HMS model: a review, Modeling Earth Systems and Environment, 9, 3029–3051, https://doi.org/10.1007/s40808-023-01704-7, 2023.

Samaniego, L., Kumar, R., and Attinger, S.: Multiscale parameter regionalization of a grid-based hydrologic model at the mesoscale, Water Resources Research, 46, 2008WR007 327, https://doi.org/10.1029/2008WR007327, 2010.

Samaniego, L., Kumar, R., Zink, M., Cuntz, M., Mai, J., Thober, S., Schneider, C., Dalmasso, G., Musuuza, J., Rakovec, O., Craven, J., Schäfer, D., Prykhodko, V., Schrön, M., Spieler, D., Brenner, J., Langenberg, B., Schüler, L., Stisen, S., Demirel, C. M., Jing, M., Kaluza, M., Schweppe, R., Shrestha, P. K., Döring, N., and Müller, S.: mhm-ufz/mHM: v5.13.4, https://doi.org/10.5281/zenodo.21670439, 2026.

Seidl, R. and Turner, M. G.: Post-disturbance reorganization of forest ecosystems in a changing world, Proceedings of the National Academy of Sciences of the United States of America, 119, e2202190 119, https://doi.org/10.1073/pnas.2202190119, num Pages: 10 Web of Science ID: WOS:000932004200001, 2022.

Shifley, S. R., He, H. S., Lischke, H., Wang, W. J., Jin, W., Gustafson, E. J., Thompson, J. R., Thompson, F. R., Dijak, W. D., and Yang, J.: The past and future of modeling forest dynamics: from growth and yield curves to forest landscape models, Landscape Ecology, 32, 1307–1325, https://doi.org/10.1007/s10980-017-0540-9, 2017.

Shugart, H. H., Wang, B., Fischer, R., Ma, J., Fang, J., Yan, X., Huth, A., and Armstrong, A. H.: Gap models and their individual-based relatives in the assessment of the consequences of global change, Environmental Research Letters, 13, 033 001, https://doi.org/10.1088/1748-9326/aaaacc, 2018.

Smith, B., Prentice, I. C., and Sykes, M. T.: Representation of vegetation dynamics in the modelling of terrestrial ecosystems: comparing two contrasting approaches within European climate space, Global Ecology and Biogeography, 10, 621–637, https://doi.org/10.1046/j.1466-822X.2001.t01-1-00256.x, _eprint: https://onlinelibrary.wiley.com/doi/pdf/10.1046/j.1466-822X.2001.t01-1-00256.x, 2001.

https://doi.org/10.5194/egusphere-2026-4918
Preprint. Discussion started: 31 August 2026

Smith, B., Wårlind, D., Arneth, A., Hickler, T., Leadley, P., Siltberg, J., and Zaehle, S.: Implications of incorporating N cycling and N limitations on primary production in an individual-based dynamic vegetation model, Biogeosciences, 11, 2027–2054, https://doi.org/10.5194/bg-11-2027-2014, 2014.

Speich, M. J. R., Zappa, M., Scherstjanoi, M., and Lischke, H.: FORests and HYdrology under Climate Change in Switzerland v1.0: a spatially distributed model combining hydrology and forest dynamics, Geoscientific Model Development, 13, 537–564, https://doi.org/10.5194/gmd-13-537-2020, 2020.

Swain, D. L., Prein, A. F., Abatzoglou, J. T., Albano, C. M., Brunner, M., Diffenbaugh, N. S., Singh, D., Skinner, C. B., and Touma, D.: Hydroclimate volatility on a warming Earth, Nature Reviews Earth & Environment, 6, 35–50, https://doi.org/10.1038/s43017-024-00624-z, 2025.

Thober, S., Cuntz, M., Kelbling, M., Kumar, R., Mai, J., and Samaniego, L.: The multiscale routing model mRM v1.0: simple river routing at resolutions from 1 to 50 km, Geoscientific Model Development, 12, 2501–2521, https://doi.org/10.5194/gmd-12-2501-2019, 2019.

Thompson, S. E., Harman, C. J., Konings, A. G., Sivapalan, M., Neal, A., and Troch, P. A.: Comparative hydrology across AmeriFlux sites: The variable roles of climate, vegetation, and groundwater, Water Resources Research, 47, https://doi.org/10.1029/2010WR009797, 2011.

Vedder, D., Fischer, S. M., Wiegand, K., and Pe'er, G.: Developing multidisciplinary mechanistic models: challenges and approaches, Socio-Environmental Systems Modelling, 6, 18 701–18 701, https://doi.org/10.18174/sesmo.18701, 2024.

Wada, Y., Wisser, D., Eisner, S., Flörke, M., Gerten, D., Haddeland, I., Hanasaki, N., Masaki, Y., Portmann, F. T., Stacke, T., Tessler, Z., and Schewe, J.: Multimodel projections and uncertainties of irrigation water demand under climate change, Geophysical Research Letters, 40, 4626–4632, https://doi.org/10.1002/grl.50686, _eprint: https://agupubs.onlinelibrary.wiley.com/doi/pdf/10.1002/grl.50686, 2013.

Wang, C., Fu, B., Zhang, L., and Xu, Z.: Soil moisture–plant interactions: an ecohydrological review, Journal of Soils and Sediments, 19, 1–9, https://doi.org/10.1007/s11368-018-2167-0, 2019.

Wei, Z., Yoshimura, K., Wang, L., Miralles, D. G., Jasechko, S., and Lee, X.: Revisiting the contribution of transpiration to global terrestrial evapotranspiration, Geophysical Research Letters, 44, 2792–2801, https://doi.org/10.1002/2016GL072235, 2017.

Winter, C., Lutz, S., Musolff, A., Kumar, R., Weber, M., and Fleckenstein, J.: Disentangling the Impact of Catchment Heterogeneity on Nitrate Export Dynamics From Event to Long-Term Time Scales, Water Resources Research, 57, https://doi.org/10.1029/2020WR027992, 2021.

Zaherpour, J., Gosling, S. N., Mount, N., Schmied, H. M., Veldkamp, T. I. E., Dankers, R., Eisner, S., Gerten, D., Gudmundsson, L., Haddeland, I., Hanasaki, N., Kim, H., Leng, G., Liu, J., Masaki, Y., Oki, T., Pokhrel, Y., Satoh, Y., Schewe, J., and Wada, Y.: Worldwide evaluation of mean and extreme runoff from six global-scale hydrological models that account for human impacts, Environmental Research Letters, 13, 065 015, https://doi.org/10.1088/1748-9326/aac547, 2018.

Zhang, Z., Zhang, L., Xu, H., Creed, I. F., Blanco, J. A., Wei, X., Sun, G., Asbjornsen, H., and Bishop, K.: Forest water-use efficiency: Effects of climate change and management on the coupling of carbon and water processes, Forest Ecology and Management, 534, 120 853, https://doi.org/10.1016/j.foreco.2023.120853, 2023.

Zink, M., Samaniego, L., Kumar, R., Thober, S., Mai, J., Schäfer, D., and Marx, A.: The German drought monitor, Environmental Research Letters, 11, 074 002, https://doi.org/10.1088/1748-9326/11/7/074002, 2016.